DOI: https://doi.org/10.37434/tpwj2025.04.06

TECHNOLOGICAL STRENGTH OF 25KhN3MFA STEEL JOINTS IN SUBMERGED ARC WELDING

A.K. Tsaryuk, V.Yu. Skulskyi, V.P. Yelagin, I.G. Osipenko

E.O. Paton Electric Welding Institute of the NASU
11 Kazymyr Malevych Str., 03150, Kyiv, Ukraine

ABSTRACT

Weldability of 25KhN3MFA steel was studied and requirements for the possibility of its application in manufacture of welded structures in heavy mechanical engineering were established. Investigations of weldability of 25KhN3MFA steel showed that hot and cold cracks form during welding of this steel. To prevent cold cracking in the welded joints, welding should be performed with preheating and interpass heating up to 250–300 °C and mandatory post-weld tempering at 570 °C. Hot cracks form in welding the root layer of the weld metal, which is related to a significant fraction of the base metal (> 50 %) at mixing with the deposited metal. To enable manufacturing welded structures from this steel, it is necessary to use only automatic narrow-gap submerged arc welding and to remove the root layer from the inner side of a welded joint. When it is impossible to remove the root weld, welded structures from 25KhN3MFA steel are not allowed for operation.

KEYWORDS: complex-alloyed steels, narrow-gap submerged arc welding, weldability, cold cracks, hot cracks, preheating and interpass heating, structure

INTRODUCTION

For the manufacture of large-sized thick-walled structures in heavy engineering, complex-alloy Cr–Ni–Mo body steels of 20KhNMFA, 20KhN3MA, 25KhN3MFA type, etc. are used [1]. These steels have the required ductility and toughness at high values of strength after appropriate heat treatment. However, their susceptibility to hardening and a high level of mechanical properties cause a number of difficulties in their welding. This primarily concerns the formation of hot and cold cracks and the production of equally strength welded joints [2]. To solve this problem, it is necessary not only to correctly set the thermal mode of welding and select welding consumables, but also to choose the correct welding method that ensures the quality of welded joints. At manufacturing of the first hydraulic cylinder bodies of 20KhN3MA steel for presses with a capacity of 30 thou t at PJSC NKMZ (Kramatorsk), electroslag welding (ESW) was the main welding method. However, the cylinders produced using ESW were not reliable enough. During operation under variable load conditions, cracks formed in the welded joints, which caused fracturing of the hydraulic cylinders. The nature of these cracks is largely determined by the specifics of the ESW process. The causes of defects and disadvantages of ESW of complex-alloyed steels were studied in [3–5].

Studies of full-scale models of hydraulic press cylinder bodies made by ESW and narrow-gap submerged arc welding of 20KhN3MA steel have shown that the most challenging welding method is automatic narrow-gap submerged arc welding. This method [6, 7] ensures a minimal penetration of the welded edges and dilution of the weld metal with the base metal, a narrow heat-affected zone, homogeneity of chemical composition and mechanical properties along the height of the edge preparation, a limited volume of deposited weld metal at its fine-grained structure and minimal residual stresses and strains. In addition, unlike ESW, in narrow-gap submerged arc welding, a single high tempering provides a sufficiently complete reduction of residual stresses and improves the structure and properties of welded joints. At the same time, high-temperature heat treatment is required after ESW, and for complex-alloyed steels, in several stages [6].

Thus, narrow-gap submerged arc welding of massive thick-walled products made of complex-alloyed steels not only ensures high quality welded joints with high process efficiency, but also is one of the reserves of energy saving, which is very important at the present time.

For the manufacture of hydraulic cylinders for pressing equipment, it is necessary to use large-sized cylindrical forged billets of thick metal (≥ 500 mm thick) made of high-strength steels welded with girth welds. In this case, 25KhN3MFA steel can be considered a promising option, as a high carbon (0.25 %) and nickel (more than 3.5 %) content ensures a sufficient hardenability throughout the entire thickness, which contributes to the stability of the strength values and service properties of thick metal. However, information on the technological strength of welded joints of this steel is very limited.

Table 1. Chemical composition of the studied steel and metal deposited using the applied welding wire, wt.%

Steel/wire grade	C	Si	Mn	Cr	Ni	Mo	V	S	P
								Not more than	
Steel									
25KhN3MFA TU 108.11.917–87	0.20–0.25	0.17–0.37	0.20–0.50	1.40–1.80	3.00–3.75	0.30–0.50	0.08–0.15	0.020	0.020
25KhN3MFA	0.25	0.26	0.36	1.60	3.50	0.33	0.15	0.020	0.020
Wire									
Sv-08KhN2GMYu GOST 2246–70	0.06–0.11	0.25–0.55	1.00–1.40	0.70–1.10	2.00–2.50	0.40–0.65	–	0.030	0.030
Sv-08KhN2GMYu	0.11	0.31	0.95	0.80	2.00	0.60	–	0.02	0.025

THE AIM

of this study was to investigate the weldability of 25KhN3MFA steel and determine the possibility of its using for critical welded structures in heavy engineering.

MATERIALS AND METHODS FOR EXPERIMENTS AND RESEARCH

The chemical composition of 25KhN3MFA steel is shown in Table 1. To produce welded joints, a combination of Sv-08KhN2GMYu wire (Table 1) and AN-17 flux [8] was used, which finds its application in power engineering for the manufacture of products from low-alloy steels.

The regularities of forming the structure of 25KhN3MFA steel depending on the thermal conditions of welding were studied using the experimentally obtained continuous cooling transformation (CCT) diagram [9]. To model the corresponding structural changes and simulate the thermal cycles of welding, a high-speed dilatometer of the PWI design was used. In the experiments, the special test specimens were heated to a temperature of 1300–1350 °C, followed by cooling in accordance with the thermal cycles of manual welding, automatic submerged arc welding (with and without preheating), electroslag welding, and welding with significant heat removal. The cooling time was counted down from the A_{C3} temperature determined in advance using a Chevenard dilatometer. After the specimens had cooled completely, metallographic analysis and hardness measurements were performed.

Microstructural examinations were performed in the Neophot-32 light microscope equipped with an Olympus P-5060 optical module with computer-controlled image capture. The microstructure in polished sections was revealed by electrolytic etching in a 10 % aqueous (distilled water) solution of chromic acid at the following conditions: voltage 12–15 V, etching time 10–15 s; in the process of preparing microsections, the etched surfaces were repolished on the cloth with the application of powdered chromium oxide. A 30 % solution of iron chloride ($FeCl_3$) was used to etch the macrosections of welded joints. The Vickers hardness was measured using a TP-5 hardness tester at a load of 10 kg.

For a qualitative assessment of the susceptibility of welded joints to cracking, butt joints of the type of technological samples of the Lehigh University ("L" sample) [10] with a modified edge configuration - from U- to X-shaped were used (Figure 1). The sample design elements were corrected to enable submerged arc welding, since the original "L" sample was designed for manual arc welding. The tests were carried out at different preheating temperatures, but under constant welding conditions: 2.0 mm diameter wire, one-sided welding, I_w = 320–340 A, U_a = 36–38 V, V_w = 18 m/h. The cooling rate was set by the preheating temperature in the range of 20–300 °C. For each preheating temperature, 3 specimens were welded.

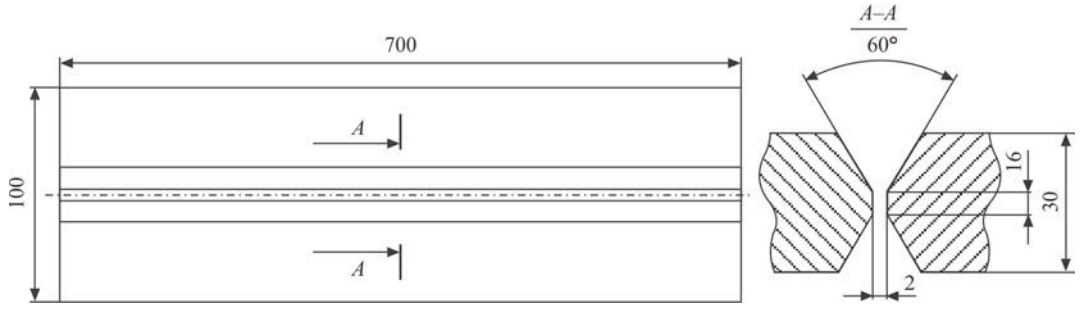

Figure 1. Technological sample

The preheating temperature sufficient to prevent cold cracking was estimated based on the analysis of the constructed thermokinetic diagram of austenite transformation.

RESEARCH RESULTS AND THEIR DISCUSSION

Typically, the weldability of hardening steels before welding is assessed by analysing their response to the thermal deformation cycle of welding and the nature of the formed phases. Such regularities are described by the results of dilatometric studies. Thus, Figure 2 shows the CCT diagram of 25KhN3MFA steel, constructed at cooling rates in the range of 600–500 °C ($w_{6/5}$) within 0.3–100 °C/s.

In the initial state, the microstructure of the tempered steel consists mainly of sorbite (Figure 3, *a*) with a hardness of *HV* 246. When heating to the austenitic state and cooled within the specified range of cooling rates, the phase transformation can occur

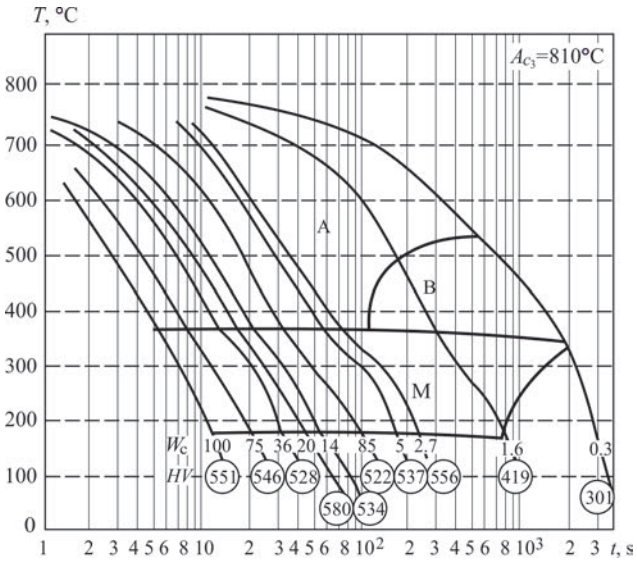

Figure 2. CCT diagram of 25KhN3MFA steel

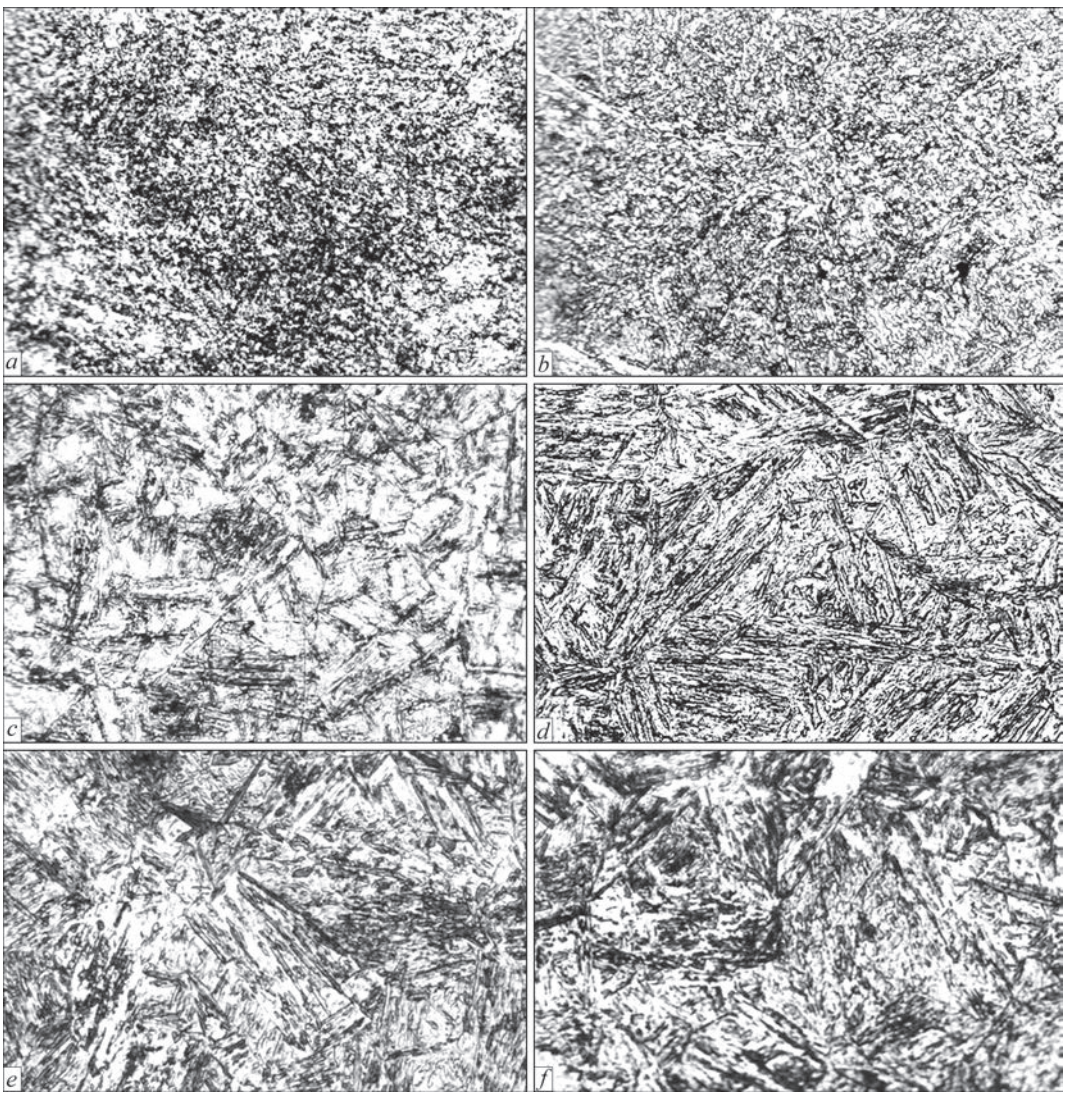

Figure 3. Microstructure of 25KhN3MFA steel after modeling different thermal cycles: *a* — initial state; *b* — $w_{6/5}$ = 0.3 °C/s; *c* — 1.6; *d* — 2.7; *e* — 20; *f* — 100 (×300)

in the bainitic and martensitic regions. No ferrite or pearlite transformation was observed.

At a cooling rate of 0.3 °C/s, a predominantly single-phase bainitic transformation occurs with the formation of granular bainite (Figure 3, *b*). With an increase in the cooling rate from 0.3 to ~2.7 °C/s, the transformation takes place both in the bainitic and martensitic regions and is accompanied by an increase in hardness from *HV* 419 to 556. The structure typical of this range, obtained at $w_{6/5}$ = 1.6 °C, is shown in Figure 3, *c*: the structural components are lamellar bainite and martensite. At $w_{6/5} \geq 2.7$ °C/s, only martensitic transformation occurs with the formation of acicular martensite (Figure 3, *d–i*); the hardness level remains high in the entire range of applied cooling rates ($w_{6/5}$ = 2.7–100 °C/s) and is approximately *HV* 520–580.

An approximate estimate of the steel susceptibility to cold cracking during welding can be performed based on the results of studying the temperature of end of martensitic transformation at different cooling rates in terms of hardness level, as well as the value of carbon equivalent C_E determined with regard to chemical composition. For example, in this case, the IIW expression can be used [11], developed for low-alloy steels with alloying limits that are close to those of the studied steel:

$$C_E = C + \frac{Mn}{6} + \frac{Cr + Mo + V}{5} + \frac{Cu + Ni}{15}, \%.$$

It is assumed that if C_E is higher than 0.40 %, there is a risk of cold cracking. For 25KhN3MFA steel with the actual composition given in Table 1, the calculation gives C_E = 0.97 %, which indicates the probability of crack formation in welded joints. However, this index has a drawback, as it does not take into account the behaviour of steel during welding [11]. It is also generally accepted that steel is prone to cold cracking when martensitic transformation ends at temperatures below 300 °C and the hardness of the transformation products exceeds *HV* 350–360 [12–14].

The analysis of the thermokinetic diagram of the transformation of austenite in 25KhN3MFA steel shows that at cooling rates $w_{6/5}$ = 1.6–100 °C/s, the end temperature of the martensitic transformation is in the range of 170–180 °C. Only at $w_{6/5}$ = 0.3 °C/s, at which partial martensite formation was still observed, the end temperature of martensitic transformation grew to 320 °C, and the hardness of the transformation products decreased to *HV* 300.

In real welding, the cooling rate of the welded joint metal may be slightly higher than the minimum rate obtained in dilatometric experiments. The approximate cooling rate can be estimated using analytical equations from the theory of welding thermal processes; to calculate the instantaneous cooling rate, the equation of the following type was used [15]:

$$w = 2\pi\lambda[(T–T_0)^2/(q/v)],$$

where w is the cooling rate when the bead is deposited on the surface of a massive body (the calculation scheme is chosen taking into account the probable heat dissipation during welding of a thick-walled product); λ is the thermal conductivity coefficient; T and T_0 are the temperature for which w is calculated and the initial temperature of the steel; v is the welding speed; $q = \eta IU$ is the thermal power of the welding arc, which is determined by the product of the effective heating efficiency of a part by the arc (η), welding current (I) and voltage (U).

For the calculations, the values of η = 0.9 (for submerged arc welding) and $\lambda \approx 30$ W/(m·°C) (according to the data for 30KhN2MFA steel, which is similar in alloying) were chosen. For a temperature of T = 550 °C, which is an average in the range of 600–500 °C, and an initial heating temperature of T_0 = 200, 300 and 350 °C, the following values of the average cooling rate $w_{6/5}$ were obtained:

- 10.5 °C/s at preheating up to 200 °C;
- 5.4 °C/s at preheating up to 300 °C;
- 3.4 °C/s at preheating up to 350 °C.

At welding without preheating — $w_{6/5}$ = 24.07 °C/s.

Therefore, under submerged arc welding conditions, martensitic transformation will occur in welded joints in the range from $M_s \approx 380$ °C to $M_f \approx$ 170–180 °C with the resulting steel hardness significantly exceeding the approximate critical level of *HV* 350.

Thus, a preliminary assessment of the weldability of 25KhN3MFA steel based on the value of the calculated carbon equivalent and the analysis of austenite transformation regularities indicates a high susceptibility of its welded joints to cold crack formation. To prevent cracking in all types of mechanized welding, preheating and accompanying heating is required.

Typically, welding of complex-alloyed power engineering steels is supposed to be carried out with preheating up to 350 °C and higher. However, both preheating and a high temperature of this operation complicate the technological process. In addition, an excessive preheating temperature can lead to an increase in residual stresses and cause microstructure deterioration. From a physical and metallurgical point of view, during welding of steels with martensitic transformation, it is advisable to preheat and maintain the interpass temperature within the M_s–M_f range, giving preference to temperatures close to M_f. This approach enables martensitic transformation in the

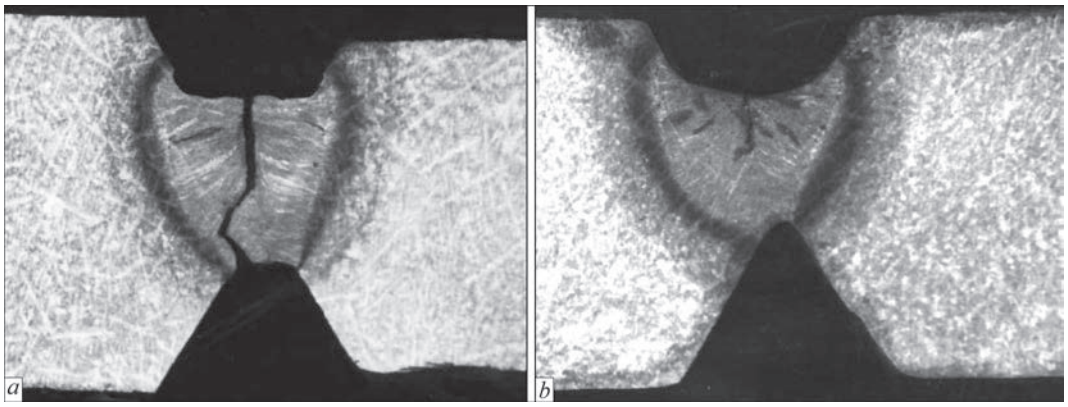

Figure 4. Solidification cracks in welds when welding samples of 25KhN3MFA steel using Sv-08KhN2GMYu wire: *a* — with a diameter of 3 mm; *b* — 2 mm

area of the last produced pass, and repeated welding heating, activating diffusion processes, causes partial martensite decomposition — tempering of hardened layers, as well as a decrease in the concentration of diffused hydrogen in them; the result is an increase in resistance to delayered fracture [16]. Limiting the preheating level also simplifies the production process itself.

It is advisable to clarify the preheating temperature by welding technological samples. Preliminary tests as well as practical experience have shown that cracks in the welded joints of 25KhN3MFA steel were mainly observed in the weld metal zone. For this reason, "L" type samples from the Lehigh University were used, the configuration of which facilitates the initiation of cracks namely in the welds.

It was experimentally established that in all cases of welding specimens without preheating and with preheating to 150, 200, 250 and 300 °C, cracks occurred in the weld zone. The cracks were detected in the hot metal immediately after the slag crust was removed.

Based on practical experience, it is known that preheating at the level of 250–300 °C is usually sufficient to eliminate cold cracks in the joints of hardening power mechanical engineering steels. In addition, their formation occurs after the end of welding and cooling of the metal, and in some cases it occurs within several tens of hours. In this case, cracks formed in the weld metal during welding and under the condition of preheating, which eliminates the probability of namely cold cracking. Therefore, it can be assumed that cracks in the welds formed during welding with preheating do not belong to cold cracks.

After a full cycle of research, it was found that cracks on 25KhN3MFA steel samples are hot cracks formed during solidification of the weld metal.

The formation of such cracks in the welds occurred under different experimental conditions. Changing the wire diameter from 2 to 3 mm in order to influence the shape of the pool and orientation of the solidification elements did not lead to positive results (Figure 4). Considering the complex alloying of the used wire, welding was performed using low-carbon Sv-08GA wire. Such a measure also did not prevent the appearance of solidification cracks. Cracks were also formed when beads were deposited on the surface of 25KhN3MFA steel, both in reverse and direct polarity (Figure 5).

Analysis of the chemical composition of the weld metal welded using Sv-08KhN2GMYu wire showed an increased carbon content (0.17–0.18 %) near the crack. The average composition of sulphur and phosphorus was within acceptable limits (S — 0.025 %, P — 0.020 %). However, metallographic examinations using local electron probe mictroanalysis re-

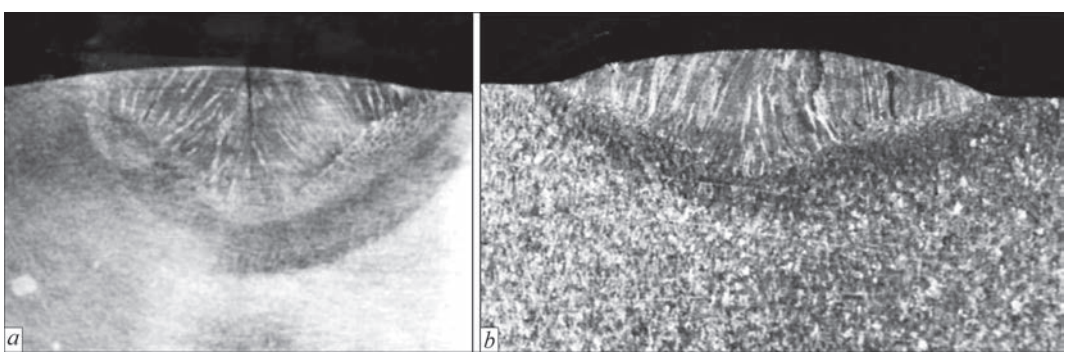

Figure 5. Solidification cracks when depositing bead on the surface of 25KhN3MFA steel using Sv-08GA wire with a diameter of 3 mm: *a* — reverse polarity; *b* — direct polarity

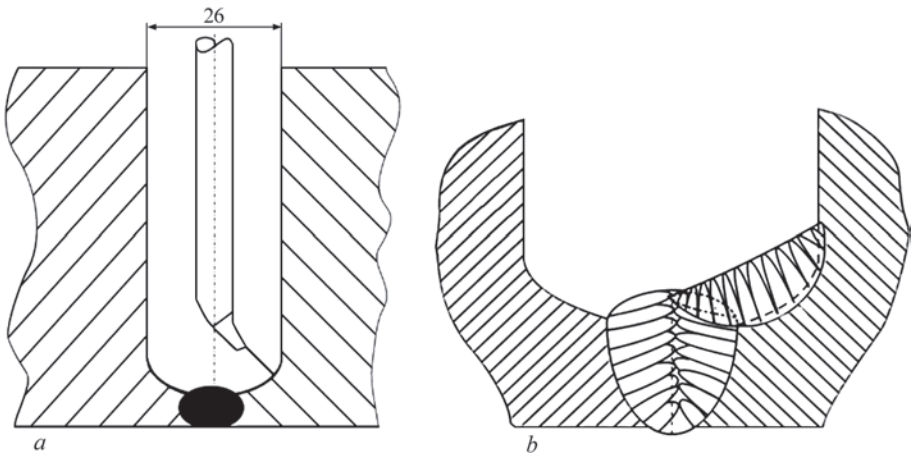

Figure 6. Layout schemes of the mouthpiece in a narrow groove (*a*) and the nature of beads solidification (*b*)

vealed segregation of sulphur and phosphorus in the area of crack initiation and propagation, which can be considered one of the factors that may contribute to the formation of such defects.

Also, an increased susceptibility of welded joints of 25KhN3MFA steel to hot crack formation can be associated with the high content of carbon and nickel in the base metal [13], which, for example, is reflected by the HCS index (Hot Cracking Susceptibility) [12]:

$$HCS = \frac{C\left(S + P + \frac{Si}{25} + \frac{Ni}{100}\right)\cdot 10^3}{3\,Mn + Cr + Mo + V}.$$

Hot cracks do not form in a welded joint if HCS < 4.0; in the case of large-thick high-strength steels, hot cracks will not form if HCS < 1.6–2.0. In our case, for 25KhN3MFA steel, HCS = 6.7, which indicates a high susceptibility of weld metal with such chemical composition to form solidification cracks.

During narrow-gap submerged arc welding of 25KhN3MFA steel, hot cracks formed in the first root layer when the arc was located at a right angle to the surface of the metal being welded. In this process, the fraction of the base metal at stirring with the deposited metal was ~50 %. At further filling of the gap with the arc orientation at an acute angle towards the edges, the penetration depth decreased (Figure 6), the fraction of the base metal also decreased, but it did not exceed the maximum level of 30 %. Under these conditions, except for the root layer, no cracks formed in the weld.

For comparison, the chemical composition of the metal of the root and filling passes was evaluated. The content of each of E_{WMi} elements in the weld was calculated as a total amount of this element transferred from the base metal and filler wire, according to the expression:

$$E_{WMi} = \Sigma(D_{PM}E_{PMi} + D_{WR}E_{WRi}),$$

where D_{PM}, D_{WR} are fractions of the base metal (*PM*) and welding wire (*WR*) at stirring in the weld (for the root pass D_{PM} and D_{WR} are assumed to be equal to 50 and 50 % and for the filling passes — 30 and 70 %); E_{PMi}, E_{WRi} are concentrations of the *i*-th element in the base metal and in the welding wire.

The approximate composition of different areas of the weld metal and the corresponding values of HCS index are shown in Table 2. For the root pass, the rounded value of HCS is ~3.8 (actually 3.778), exceeding the corresponding value for the filling passes, which was calculated to be 3. However, it should be noted that HCS ≤ 3 % should be considered for the filling passes, since for these conditions, as noted above, $D_{PM} \leq 30$ %.

As is seen from the calculation results, in both cases, HCS values were less than the critical level of HCS = 4, but cracks still occurred in the root pass. In addition, this value for the filling passes was higher than the critical value for a thick-walled joint of increased hardness (HCS = 2), although no cracks formed in the metal of the filling passes. Thus, the obtained research data indicate that there is no unambiguous explanation for the cause of solidification crack formation, which, for example, is seen from the inconsistency of welding results and evaluation of the technological strength according to HCS criterion. In general, solidification crack formation has a complex mechanism, in which both metallurgical and force factors are simultaneously manifested [13, 15]. Depending on the chemical composition, the segregation

Table 2. Results of calculated chemical composition of root and filling passes and HCS indices

Weld zones	C	Si	Mn	Cr	Ni	Mo	V	S	P	HCS
Root	0.180	0.285	0.655	1.20	2.75	0.465	0.075	0.020	0.022	3.8
Filling pass	0.152	0.295	0.773	1.04	2.45	0.519	0.045	0.020	0.021	3.022

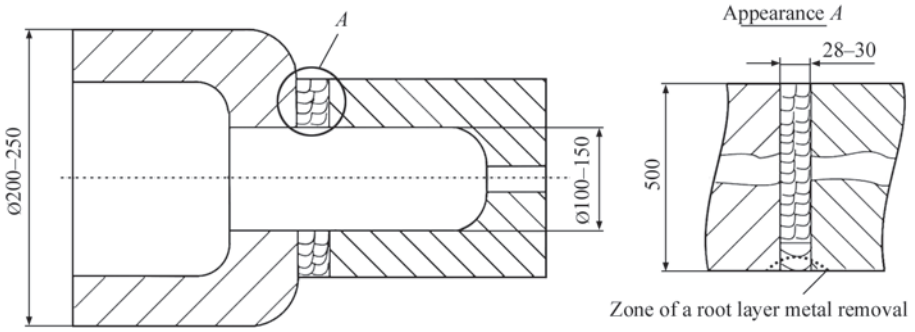

Figure 7. Scheme of a welded hydraulic press cylinder

of the most harmful impurities — S and P, or C and Ni can have a prevailed effect; in low-alloy welds which are free from impurities, the crack formation is dominated by the segregation of the latter two elements [13, 17]. According to [17], in iron-carbon welds, low technological strength was observed at approximately 0.1 % C and at C > 0.17 %. In Fe-Ni type welds, an increase in crack susceptibility occurred at Ni > 2–3 %. The role of C and Ni in the mechanism of crack formation is also associated with their influence on the nature of primary solidification [17]. The study of the combined effect of C and Ni using the concentration index Ni_{eq} (Ni_{eq} = Ni + *k*C, where *k* is a coefficient depending on the C content) showed that a significant increase in the susceptibility to solidification cracks occurred at Ni_{eq} is greater than ~3.4 %. Under this condition, the primary solidification with the formation of δ-phase (according to the L → δ scheme) transferred to the solidification of δ + γ through the peritectic reaction (L → δ + (L + δ = γ) → δ + γ). A decrease in resistance to crack formation may be a consequence of:

a) increased liquation of S and P at a decrease in their solubility in the γ-phase, in which Ni and C were also more soluble;

b) an additional (to the overall thermal reduction) increase in the level of microdeformations near the solidification boundary as a result of volumetric changes caused by the formation of the γ-phase at a two-phase solidification of δ + γ.

In the considered case of welding 25KhN3MFA steel, the weld metal, depending on the degree of stirring the base and weld metals may have a resulting C and Ni content that increases its susceptibility to solidification cracks. For example, when making root passes due to a significant fraction of the base metal (up to 50 %), the weld is enriched with carbon (up to 0.18 %). This level of carbon in the weld metal contributes to the formation of hot cracks. The segregation of harmful impurities (S, P) at their normal admissible content in steel is also an important metallurgical factor in reducing technological strength. Nickel creates an additional effect, enhancing the liquation of these elements and contributing to the formation of crack initiation sites. The negative impact of a significant dilution of the deposited metal with the base metal is also shown on the example of beads deposited on steel using Sv-08GA wire, when the fraction of the base metal was 60–80 %. In turn, a reduction in the HCS index for the filling passes relative to the root passes can contribute to an increase in crack resistance. In addition, the shape of the weld cross-section and the corresponding directions of crystallite growth during weld pool solidification are also important factors in the formation and prevention of hot cracks [13, 15]. The root pass is characterized by deep penetration relative to the width of the weld pool and trancrystalline (counter) growth of solidification elements from the pool walls. The formation of liquid enriched with impurities in the axial zone at the joining of crystallites in this pool shape contributes to the appearance of cracks under the influence of welding deformations (Figure 6).

At a wider and shallower shape of the pool with the crystallite growth directed towards the zenith and displacement of the low-melting liquid into the upper

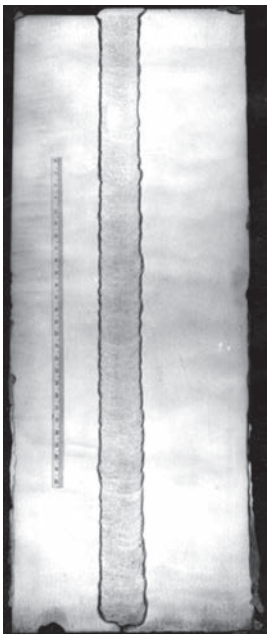

Figure 8. Macrosection of a butt joint with a weld depth of 500 mm

Table 3. Mechanical properties of welded joint of 25KhN3MFA steel, welded using Sv-08KhN2GMYu wire under AN-17 flux in the state after high tempering

Weld metal					Welded joint	
σ_t, MPa	$\sigma_{0.2}$, MPa	δ, %	ψ, %	*KCU*, J/cm^2	σ_t, MPa*	*KCU*, J/cm^{2**}
Requirements for properties of welded joints						
≥ 600	≥ 500	≥ 12	≥ 40	≥ 50	≥ 600	≥ 50
Test results						
786	583	16.6	55.6	115	633	72.0
783	575	16.3	51.0	137	735	62.0
788	583	16.6	55.6	122	705	115.0
785***	580***	16.5***	54.0***	124***	691***	83.0***

*Fracture over HAZ.
**Notch along the fusion line.
***Average value for three tests.

part, the resistance to hot cracking grows. Such solidification is characteristic of filling passes. Practicing the technology on models of industrial products confirmed the existence of the problem of hot cracking only for the root passes.

For the industrial production of the hydraulic cylinder body from 25KhN3MFA steel, it was agreed to use narrow-gap submerged arc welding, which is characterized by high efficiency and generally high quality of thick-walled joints (Figures 7, 8). However, considering that reaching a high quality of the root passes is problematic, after the groove had been completely filled, it was mandatory to remove the root layer of the weld metal by mechanical method using machine-tool (Figure 7).

To temper the hardening structures in the joint zone, maximize the removal of residual stresses and improve the ductility and toughness of the metal, a welded product is subjected to mandatory high tempering. Taking into account the existing recommendations and conducted tests, the tempering mode at a temperature of 570 °C for 30 h was selected, which provides the necessary mechanical properties of welded joints (Table 3). At the manufacturing stage and after heat treatment, it is recommended to carefully apply all methods of non-destructive quality testing.

The developed technological process of welding and heat treatment of powerful hydraulic cylinder bodies was introduced in the production of equipment intended for the manufacture of damaged elements of civilian structures and parts of weapons and equipment for the Armed Forces of Ukraine by press stamping, in particular, assemblies of long-range guns, cruise and ballistic missiles, which is relevant for the military-industrial complex of Ukraine.

CONCLUSIONS

1. It is shown that under conditions of automatic submerged arc welding of 25KhN3MFA steel using a combination of AN-17 flux and Sv-08KhN2GMYu wire, the metal in the joint zone undergoes hardening with the formation of a predominantly martensitic structure with a hardness of up to *HV* 520–580, which causes the risk of cold cracking. The elimination of cold cracks is achieved by preliminary/accompanying heating to 250–300 °C.

2. During laboratory tests and narrow-gap submerged arc welding of industrial mock-ups, it was established that for the manufacture of thick-walled products from 25KhN3MFA steel, the main problem is the formation of solidification cracks when producing root passes; at further filling of the groove, hot cracks were not observed.

3. Taking into account the results of experiments and modern theoretical provisions, it was assumed that in the considered case, the occurrence of solidification cracks has a complex nature. The main factors may include the enrichment of the weld metal with C and Ni due to an increase in the fraction of the base metal in the pool melt to 50 %, which is typical for root passes, the corresponding intensification of the processes of segregation of C, S and P with the formation of low-melting fracture sites, as well as an unfavourable shape of the pool with the transcrystalline type of growth of solidification elements. Filling passes form when the fraction of the base metal in the weld is reduced to 30 % or lower, as well as with a pool shape that is favourable for the displacement of low-melting constituent elements to its surface during solidification, which in combination causes the absence of hot cracks.

4. For the industrial manufacture of critical products from 25KhN3MFA steel with a wall thickness of up to 500 mm, the technology of automatic narrow-gap submerged arc welding was introduced, which involves the removal of a metal layer with a root pass using a machine-tool after welding the joint.

The final operation is high tempering at a temperature of 570 °C.

REFERENCES

1. Bashnin, Yu.A., Tsurkov, V.N., Korovin, V.N. (1985) *Heat treatment of large-sized products and semi-products at metallurgical works.* Moscow, Metallurgiya [in Russian].
2. Paton, B.E. (1974) *Technology of electric fusion welding of metals and alloys.* Moscow, Mashinostroenie [in Russian].
3. Makara, A.M., Kovalev, Yu.Ya., Novikov, I.V. (1972) Tears in near-weld zone during electroslag welding of structural steels. *Avtomaticheskaya Svarka,* **5**, 1–5 [in Russian].
4. Eregin, L.P., Malaj, A.E. (1978) Conditions of formation of near-weld cracks-tears in electroslag welding of chrome-nickel-molybdenum steels. *Svarochnoe Proizvodstvo,* **10**, 26–27 [in Russian].
5. Makara, A.M. (1963) *Investigation of problems of technology and metals science of welding of alloyed structural steels:* Collection. Kyiv, Izd-vo AN Ukr. SSR [in Russian].
6. Kasatkin, B.S., Tsaryuk, A.K., Levenberg, N.E., Pilipenko, N.V. (1984) Technological possibilities of narrow-gap submerged arc welding of medium-alloy thick steels. *Avtomaticheskaya Svarka,* **7**, 41–44 [in Russian].
7. Tsaruk, A.K., Skulsky, V.Yu., Moravetsky, S.I. (2016) Mechanized narrow-gap submerged arc welding of thick-walled cylindrical products. In: *Medovar Memorial — Symposium 7–10 June, Kyiv, Ukraine*, 82–90.
8. Kasatkin, B.S., Kravchenko, N.F., Ivanenko, V.D. et al. (1989) Narrow-gap submerged arc welding of thick-walled cylindrical products. *Avtomaticheskaya Svarka,* **5**, 31–35 [in Russian].
9. Lebedev, Yu.M., Kravchenko, L.P., Danilyuk, N.N. (1978) Procedure of modeling of welding thermodeformational cycles. *Avtomaticheskaya Svarka,* **12**, 31–33 [in Russian].
10. Kihara, H., Suzuki, H., Makamura, H. (1962) Weld cracking test of high strength steel and electrodes. *Welding J.,* **41**, 36–38.
11. (1992) *Steel:* A Handbook for Materials Research and Engineering. Vol. 1: Fundamentals. Springer-Verlag Heidelberg and Verlag Stahleisen m.b.H., Dusseldorf.
12. Hrivnak, I. (1984) *Weldability of steels.* Moscow, Mashinostroenie [in Russian].
13. Lippold, J.C. (2015) *Welding Metallurgy and Weldability*. Wiley & Sons.
14. (2017) *Materials for ultra-supercritical and advanced ultra-supercritical power plants*. Ed. by Augusto Di Gianfrancesco. Elsevier Ltd.
15. Sindo, Kou (2003) *Welding Metallurgy.* Second Ed. Wiley & Sons.
16. Skulsky, V.Yu., Moravetsky, S.I., Nimko, M.A. et al. (2019) Effect of reheating in multipass submerged-arc welding on delayed fracture resistance of rotor steel welded joints. *The Paton Welding J.,* **3**, 11–14. DOI: https://doi.org/10.15407/tpwj2019.03.02
17. Shankar, V., Devletian, J.S. (2005) Solidification cracking in low alloy steel welds. *Sci. and Technol. of Welding and Joining*, 10(**2**), 236–243.

ORCID

A.K. Tsaryuk: 0000-0002-5762-5584,
V.Yu. Skulskyi: 0000-0002-4766-5355,
V.P. Yelagin: 0000-0002-4335-5130,
I.G. Osipenko: 0000-0001-6645-7853

CONFLICT OF INTEREST

The Authors declare no conflict of interest

CORRESPONDING AUTHOR

A.K. Tsaryuk
E.O. Paton Electric Welding Institute of the NASU
11 Kazymyr Malevych Str., 03150, Kyiv, Ukraine.
E-mail: tsaryuk@paton.kiev.ua

SUGGESTED CITATION

A.K. Tsaryuk, V.Yu. Skulskyi, V.P. Yelagin, I.G. Osipenko (2025) Technological strength of 25KhN3MFA steel joints in submerged arc welding. *The Paton Welding J*., **4**, 37–45.
DOI: https://doi.org/10.37434/tpwj2025.04.06

JOURNAL HOME PAGE

https://patonpublishinghouse.com/eng/journals/tpwj

Received: 04.12.2024
Received in revised form: 16.01.2025
Accepted: 08.05.2025